1 Summaries of Experimental Activities

1.1 E91-011

Investigation of the $N \to \Delta$ Transition via Polarization Observables in Hall A

S. Frullani, J.J. Kelly, and A.J. Sarty, Spokespersons,
and
the Hall A Collaboration.

Recoil polarization observables can provide new insight into properties of nucleon resonances and the reaction mechanisms for electroproduction of mesons by providing access to interference between small amplitudes and dominant amplitudes. The dominant amplitude for pion electroproduction at the Δ resonance is the M_{1+} multipole, but there is much current interest in the smaller S_{1+} amplitude that arises from configuration mixing within the quark core [1], often described as quadrupole deformation, or from meson and gluon exchange currents between quarks [2], or coupling to the pion cloud outside the quark core [3,4]. Observables which depend upon real parts of interference products are sensitive to these quadrupole amplitudes, but reliable interpretation of such data requires understanding background contributions from nonresonant production mechanisms and from underlying nondominant resonances. Sensitivity to background amplitudes is provided by observables which depend upon the imaginary parts of similar interference products. Experiment 91-011 was designed to measure both types of observables for the $p(\vec{e}, e'\vec{p})\pi^0$ reaction using the focal-plane polarimeter.

The experiment ran between May 19 and July 31, 2000 and received an average current of 45 μA for 36.5 days, corresponding to about 64% of scheduled calendar time. The beam polarization for several cathode spots varied between 67 and 79% and was monitored almost continuously by the Compton polarimeter. Polarized beam was delivered to Hall A during the June 8 to July 1 period using two lasers and achieved a record current of 110 μA with high polarization, although the lifetime was relatively short.

The production kinematics are summarized in Table 1. The nominal beam energy, $E_0 = 4.535$ GeV, electron scattering angle, $\theta_e = 14.09^\circ$, and scattered electron momentum, $k_f = 3.066$ GeV/c, were constant for the production data. The proton momenta and angles were chosen to give central values of $W = 1.232$ GeV and $Q^2 = 1.0$ (GeV/c)^2 while optimally covering the center-of-mass angular distribution. The table lists nominal center-of-mass angles θ_{cm} where positive (negative) angles refer to nucleon momenta forward (backward) with respect to the virtual photon momentum $\vec{q}$. The total charge collected for each setting is given in coulombs. For each setting, a portion of the data was collected with 6 msr collimators in each spectrometer, but for most settings the bulk of the data was acquired without collimators. Extensive measurements for optics, pointing, luminosity, and dead time were made also.

Table 1: Kinematics summary.

θ_{cm} deg.	θ_{lab} deg.	p_{lab} GeV/c	charge C
-155	49.72	0.742	11.5
-135	53.64	0.819	20.2
-90	54.79	1.066	13.7
-50	50.18	1.270	10.5
-25	46.33	1.350	4.6
0	42.30	1.378	16.7
25	38.12	1.350	6.2
50	34.29	1.270	13.0
90	29.81	1.066	12.0
135	30.81	0.819	11.1
155	34.71	0.742	11.1
180	42.28	0.703	3.8

The high singles rates on the forward of side of $\vec{q}$ and relatively large π^+ contamination necessitate careful particle identification and background rejection. Fig. 1 illustrates the effectiveness of several selection criteria. A cut on the correlation between vertex position and coincidence time eliminates most of the accidental coincidences. A cut on mean pulse height in the scintillators versus β eliminates most of the pion contamination. An aerogel detector was used for most of the forward-angle running to reduce the trigger rate and dead time contributed by pions. An additional cut on missing energy versus missing mass also reduces background, particularly on the large-angle side of $\vec{q}$ where the elastic radiative tail is responsible for the strong peak at small missing mass; this peak is cut off on its lower side by acceptance. Very little background remains under the final missing-mass peak. Note that the missing-mass resolution is better on the large-angle than on the small-angle side of $\vec{q}$ where the sensitivity to angular resolution is greater.

Even though the hadron spectrometer is confined to a horizontal plane, Fig. 2 demonstrates that kinematic focussing of the reaction cone to a laboratory opening angle of about 13° provides considerable out-of-plane acceptance. The nearly complete coverage for $\theta_{cm} < 50°$ will permit extraction of response functions which require out-of-plane momenta. Therefore, we have developed an analysis procedure that exploits the various ϕ dependencies of cross section and polarization observables to extract most of the response functions that do not require Rosenbluth separation. This procedure was tested by Monte Carlo simulation before the experiment and will be applied to the data after completion of the necessary calibration tasks. The data analysis is proceding smoothly and we expect to have preliminary data for polarized and unpolarized response functions by Spring of 2001.

References

[1] N. Isgur, G. Karl, and R. Koniuk, Phys. Rev. D **25**, 2394 (1982).

[2] A.J. Buchmann, hep-ph/9909385 (1999).

[3] M. Fiolhais, B. Golli, and S. Sirca, Phys. Lett. **B373**, 229 (1996).

[4] S.S. Kamalov and S.N. Yang, Phys. Rev. Lett. **83**, 4494 (1999).

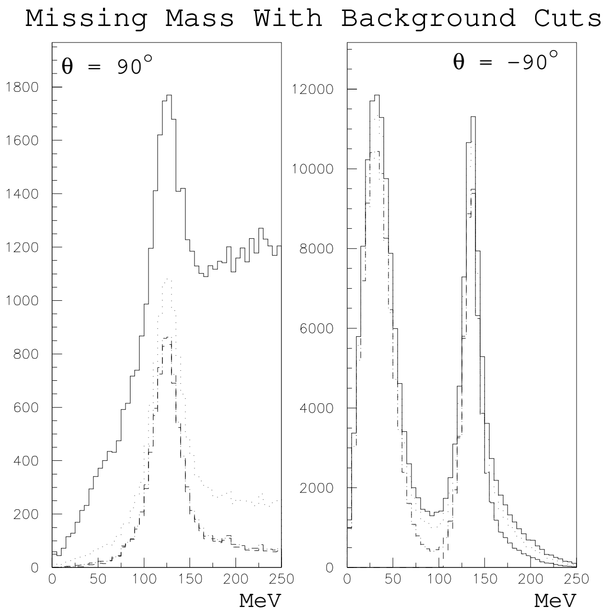

Figure 1: The effectiveness of event selection criteria is illustrated for $\theta_{cm} = \pm 90°$. The solid curves are uncut, close-dotted curves are cut on coincidence time, dash-dotted curves add a vertex cut, wide-dotted curves add the β versus pulse-height particle identification, and the dashed curve selects pion production in E_m versus p_m.

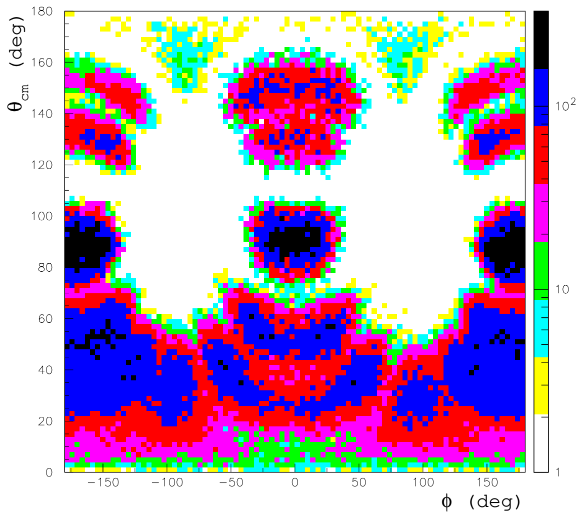

Figure 2: Angular acceptance for $1.207 \leq W \leq 1.257$ GeV and $0.9 \leq Q^2 \leq 1.1$ (GeV/c)^2. Contours of normalized yield are shown for (θ_{cm}, ϕ_{cm}), combining the various spectrometer settings.